Polymer 51 (2010) 3956–3965

Contents lists available at ScienceDirect

Polymer

journal homepage: www.elsevier.com/locate/polymer

Using organoclay to promote morphology refinement and co-continuity in high-density polyethylene/polyamide 6 blends – Effect of filler content and polymer matrix composition

G. Filippone [a,*], N.Tz. Dintcheva [b], F.P. La Mantia [b], D. Acierno [a]

[a] Dipartimento di Ingegneria dei Materiali e della Produzione, Università di Napoli Federico II, Piazzale V. Tecchio, 80, 80125 Napoli, Italy
[b] Dipartimento di Ingegneria Chimica dei Processi e dei Materiali, Università di Palermo, Viale delle Scienze, Ed. 6, 90128 Palermo, Italy

ARTICLE INFO

Article history:
Received 2 March 2010
Received in revised form
6 May 2010
Accepted 23 June 2010
Available online 30 June 2010

Keywords:
Nanocomposite
Immiscible blends
Microstructure

ABSTRACT

We investigate the gradual changes of the microstructure of two blends of high-density polyethylene (HDPE) and polyamide 6 (PA6) at opposite composition filled with increasing amounts of an organo-modified clay. The filler locates preferentially inside the polyamide phase, bringing about radical alterations in the micron-scale arrangement of the polymer phases. When the host polyamide represents the major constituent, a sudden reduction of the average sizes of the polyethylene droplets was observed upon addition of even low amounts of organoclay. A morphology refinement was also noticed at low filler contents when the particles distributes inside the minor phase. In this case, however, keep increasing the organoclay content eventually results in a high degree of PA6 phase continuity. Rheological analyses reveal that the filler loading at which the polyamide assembles in a continuous network corresponds to the critical threshold for its rheological transition from a liquid- to a gel-like behaviour, which is indicative of the structuring of the filler inside the host PA6. On the basis of this finding, a schematic mechanism is proposed in which the role of the filler in driving the space arrangement of the polymer phases is discussed. Finally, we show that the synergism between the reinforcing action of the filler and its ability to affect the blend microstructure can be exploited in order to enhance relevant technological properties of the materials, such as their high temperature structural integrity.

1. Introduction

A considerable portion of the market of plastic materials is dominated by a limited number of commodity polymers. Nevertheless, the increasing demand of materials for advanced applications or characterized by specific combination of properties cannot be satisfied by simple homopolymers. This explains the considerable scientific and industrial interest in modifying or mixing these commodity polymers, aimed at achieving performances currently exhibited solely by expensive engineering resins or non-polymeric materials [1]. Blending different polymers and yet conserving their individual properties in the final mixture is an attractive and inexpensive way of obtaining new polymeric materials [2]. The entropy of mixing of polymers is usually very low, so polymer mixtures tend to phase separate. As a consequence, besides the properties of the single constituents, the micron-scale arrangement of the phases plays a major role in determining the final properties of a polymer blend. In binary mixtures immiscibility usually results in globular morphologies, where spheroidal droplets of the minor phase are suspended in a matrix constituted by the major constituent. Generally, the properties of such systems range between those of the neat constituents, but in some case they can be governed by one of them. For example, the mechanical strength of droplets-matrix blends is essentially controlled by the matrix, and its fracture toughness can result drastically worsened if a poor interfacial adhesion exists between the constituents. A particular arrangement of the phases known as co-continuity can be achieved within a narrow range of compositions and using appropriate expedients during the mixing process. The distinguishing feature of co-continuous morphologies is the mutual interpenetration of the phases, which is often desirable as it may result in a remarkable combination of functional and structural properties of the blend constituents [3–5]. In addition, co-continuous morphologies allow the removal of one phase, which results in porous, high-surface-area structures that can be used in a wide range of applications, including separations, catalysis, and templating [6].

Co-continuity can be achieved through the quenching of non-equilibrium morphologies produced during intense mechanical

* Corresponding author. Tel.: +390817682407; fax: +390817682404.
E-mail address: gfilippo@unina.it (G. Filippone).

0032-3861/$ – see front matter © 2010 Elsevier Ltd. All rights reserved.
doi:10.1016/j.polymer.2010.06.044

mixing [7,8]. However, preserving the finely interpenetrated structure attained during the processing stage is difficult, and the material quickly moves toward equilibrium loosing its co-continuity. One solution is the using of compatibilizing agents such as copolymers, either deliberately added or formed *in situ*, which help to control coalescence phenomena and improve the adhesion between the two-phases. Copolymers need to be chemically tailored to a specific polymer pair, thus restricting their use to a relatively small number of systems. As a consequence, a remarkable scientific and technological interest exists aimed at identifying more general routes for the morphological stabilization of co-continuous polymer blends. In the last years it has been proposed to substitute the traditional compatibilizing agents with small amounts of nanometric particles [9]. More generally, the using of nanoparticles has revealed as a viable route for manipulating the nano- and microstructure of multiphase polymeric materials, imparting them novel properties. Typically, one of the polymer preferentially adsorb onto the particles. Hence, the motion of the particles influences the behavior of the polymeric fluids, and the structural evolution of the latter in turn affects the dispersion of the particles. As a consequence, it has been widely reported in the literature that small amounts of nanoparticles radically affect the microstructure of immiscible polymer blends, either causing a drastic size reduction of the minor phase [10–15] or shifting the composition at which co-continuity occurs [16–21]. As for low viscosity fluid emulsions, the knowledge of the polymer/polymer and polymer/filler interfacial tensions should be sufficient to predict the distribution of the filler in a polymer blend. Mere wettability considerations, however, allow predicting the localization of the filler only provided that thermodynamic equilibrium is attained. This condition is generally not verified in polymer blends during mixing because of the high viscosity of the polymer melts, and processing parameters such as the temperature, intensity and duration of mixing, as well as the sequence of addition of the constituents, become additional factors affecting the uneven distribution of nanoparticles in polymer blends [22]. In spite of the high complexity of the physical mechanisms behind the irregular distribution of the filler, it is widely recognized that adding nanoparticles to polymer systems with an existing phase-separated morphology represents an elegant way to promote new properties and optimized behaviors, which are otherwise absent in the unfilled matrices [23].

In a recent paper we investigated the effect of an organomodified montmorillonite on the morphology and properties of a blend of high-density polyethylene (HDPE) and polyamide 6 (PA6) at a weight ratio HDPE/PA6 75/25 [24]. Polyethylene is used in a large field of applications ranging from packaging to adhesives and wire coatings, but its employ in the automotive and construction industries is limited by the low melting temperature and poor heat resistance. As a consequence, polyethylene is often blended with a high-melting-temperature polymer such as polyamide [25]. However, since such blends tend to phase separate on the macroscopic scale, a substantial improvement of thermal and mechanical properties can be achieved only when the polyamide phase is continuous. Therefore, a challenging task is promoting a co-continuous microstructure, where the polyamide may form a stress bearing framework able to resist above the polyethylene softening temperature while keeping the polyolefin as the major constituent. By combining different experimental techniques such as wide-angle X-ray diffractometry, differential scanning calorimetry, selective extraction experiments, thermogravimetrical analyses and rheological measurements, in our previous paper we found that Cloisite® 15 A tends enriching the polyamide phase of HDPE/PA6 blends [24]. The uneven distribution of the filler brings about drastic changes in the microstructure of the blends, promoting a fine co-continuous morphology in spite of the low amount of polyamide. In this paper we try to gain further insight on the nature of this unexpected phenomenon by studying the gradual changes of the morphology of two HDPE-PA6 blends at opposite composition with varying the organoclay content. Possible relationships between microstructural changes and rheological behavior of the phases are investigated, and a schematic mechanism is proposed in which the role of the filler in driving the space arrangement of the polymer phases is discussed. Finally, the dynamic-mechanical behavior of the blends is studied, focusing on the impact of microstructural changes on the high temperature performances of the materials.

2. Experimental

2.1. Materials and blend preparation

The polymeric constituents of the samples are a high-density polyethylene (HDPE, Eraclene® MP94 from *Polimeri Europa*, Italy), with density $\rho = 0.96$ g/cm^3 at 23 °C and $MFI_{190\,^\circ C/2.16\ kg}$ of 7.0 g/10′, and a polyamide 6 (PA6, Radilon® S from Radici Group, Italy), with $\rho = 1.13$ g/cm^3 and intrinsic viscosity of 1.5 dL/g measured at 30 °C in 80 vol-% formic acid. The filler used is an organomodified clay supplied by Southern Clay Products with trade name of Cloisite® 15A, that is a montmorillonite modified by dimethyl–dihydrogenated tallow-quaternary ammonium cation with concentration of the organomodifier of 125 meq/100 g clay and density $\rho = 1.66$ g/cm^3.

The blends were prepared by melt compounding the constituents using a co-rotating intermeshing twin-screw extruder (OMC, Italy) equipped with a cylindrical capillary die (diameter 1.5 mm, length 15 mm). The polymers and the filler were added simultaneously in the extruder. The PA6 and the clay were dried under vacuum for 16 h at 90 °C before the extrusions. The thermal profile was 140 °C–200 °C–240 °C–240 °C–240 °C–220 °C, and the screw speed was set to ~60 rpm, corresponding to residence times of order of ~150 s. The extruded pellets, cooled in water at the die exit, were compression-molded into ~1.2 mm thick plates from which we cut the samples for the subsequent analyses. A Carver laboratory press was used for this purpose, applying a pressure of ~150 bar for 2 min at a temperature of 255 °C. The neat polymers used as reference materials were prepared under the same conditions.

The designations and compositions of the samples are reported in Table 1. As the filler enriches preferentially the polyamide phase

Table 1
Designation and composition of the blends.

Sample	HDPE/PA6 wt/wt	Clay [phr]	Clay/PA6 ratio
PA25	75/25	–	–
PA25 + lClay	75/25	0.25	0.01
PA25 + 2.5Clay	75/25	0.625	0.025
PA25 + 5Clay	75/25	1.25	0.05
PA25 + 20Clay	75/25	5	0.2
PA75	25/75	–	–
PA75 + lClay	25/75	0.75	0.01
PA75 + 2.5Clay	25/75	1.875	0.025
PA75 + 5Clay	25/75	3.75	0.05
PA75 + 20Clay	25/75	15	0.2
PA + 1Clay	0/100	1	0.01
PA + 2.5Clay	0/100	2.5	0.025
PA + 5Clay	0/100	5	0.05
PA + 20Clay	0/100	20	0.2
HDPE + 5Clay	100/0	5	–

of filled systems, PA6-based nanocomposites were also prepared using the same PA6/Clay ratios of the nanocomposite blends.

2.2. Characterization methods

The morphology of the filled samples on nanoscale was inspected through transmission electron microscopy (TEM) using a Philips EM 208 TEM with 100 keV accelerating voltage. The specimens were in the form of thin slices (thickness ~150 nm) microtomed at room temperature using a diamond knife.

Wide-angle X-ray analyses (WAXD) were performed at room temperature in the reflection mode on a Siemens D-500 X-ray diffractometer with Cu Kα radiation of wavelength of 1.54 Å, using a scanning rate of 10° min^{-1}. The interlayer spacing between the silicate layers of the organoclay, d_{001}, was computed by applying the Bragg's condition to the low-angle peak ($2° < 2\theta < 4°$) of the scattering intensities.

The microstructure of the blends was examined through scanning electron microscopy (SEM) using a SEM Leica 420. The inspected cryo-fractured surfaces of the samples were coated with a thin layer of gold. In some cases, the samples were etched with selective solvents in order to emphasize the contrast between the phases. Specifically, formic acid was used to remove the minor polyamide phase from the HDPE-based blends, while the polyethylene was etched from the surface of the blends with PA6 as the major constituent through Soxhlet extraction with boiling toluene. The selectivity of these solvents was ascertained by verifying that the neat polymers were not swelled by the respective non-solvents.

Image analysis of the SEM micrographs was performed using a public domain Java image processing program (ImageJ 1.42q). Once manually traced the phase boundaries, an equivalent size for each inclusion of the minor phase was estimated as $d_i = \sqrt{4A_i/\pi}$, where A_i is the area of the i-th drop. Then, the average size of the minor phase was evaluated as $D_v = \sum_{i=1}^{N} n_i d_i^4 / n_i d_i^3$, where n_i is the number of drops with size d_i. Moreover, in order to quantify the irregularity of the shape of the minor phase, an average circularity parameter was estimated as $C = 4\pi/N \sum_{i=1}^{N} A_i/p_i^2$, where p_i is the perimeter of the i-th drop. Each blend micrograph contained an number N of inclusions of the minor phase of several hundreds.

Quantitative extraction experiments were performed in order to estimate the degree of phase continuity of the minor constituent of the blends. Three disks (diameter 25 mm, thickness 1.2 mm) for each composition, previously weighed, were immersed into the selective solvent for the minor polymeric constituent of the blend. Once dried, the samples were weighed again and the weight loss was recorded. The procedure was repeated until a constant mass was attained. Hence, the extent of phase continuity of the soluble polymer i, φ_i, was evaluated as $\varphi_i = (m_{i0} - m_{if})/m_{i0}$, where m_{i0} and m_{if} represent the nominal masses of the extractable polymer phase in the blend before and after the extraction experiments, respectively [26]. All the samples remained self-supporting at the end of the extractions. The estimates of φ_i were computed by assuming that all the filler locates inside the polyamide phase of the blends. However, the amount of organoclay effectively removed during the experiments is actually unknown, and a fraction of particles could either remains trapped inside the sample, or it could be dragged off during the tests. Although this brings about some uncertainty on the estimates of φ_i, we ascertained that the main conclusions we drawn from the quantitative extraction experiments were not invalidated because of the relatively small amount of filler present in the studied samples.

A stress-controlled rotational rheometer was used for rheological experiments (mod. ARG2 by TA Instruments) in parallel plates geometry (plate diameter 25 mm). The measurements were performed at $T = 240$ °C in dry nitrogen atmosphere to prevent thermo-oxidative degradation. Oscillatory experiments were carried out using a strain amplitude $\gamma = 1\%$, which ensures to be in the linear regime as verified through preliminary linearity check tests. Steady-state shear tests were performed from $\dot{\gamma} = 0.1 s^{-1}$ up to ~30 s^{-1}, higher shear rates being not probed due to the occurrence of melt fracture phenomena.

Dynamic-mechanical analyses (DMA) were carried out using a Tritec 2000 DMA (Triton technology, UK). The dynamic moduli were measured as a function of temperature in single cantilever bending mode at a frequency $\omega = 1$ Hz and total displacement of 0.05 mm, which is small enough to be in the linear regime. The sample bars (sizes ~15 × 10 × 1.2 mm^3) were heated at 2 °C min^{-1} from about −90 °C to either ~140 °C or ~200 °C depending on their composition.

3. Results and discussions

3.1. Morphological analyses

In the case of blends where a polar polymer is blended with a hydrophobic one, the filler generally distribute in the former due to more favorable polymer–particle interaction [22]. This agrees with what we reported in our previous paper, in which the preferential placement of the organoclay inside the more hydrophilic PA6 phase of the blends was demonstrated by combining several targeted morphological analyses [24]. The TEM micrographs showing such uneven distribution of the filler are reported in Fig. 1 for the samples PA25 + 20Clay and PA75 + 5Clay.

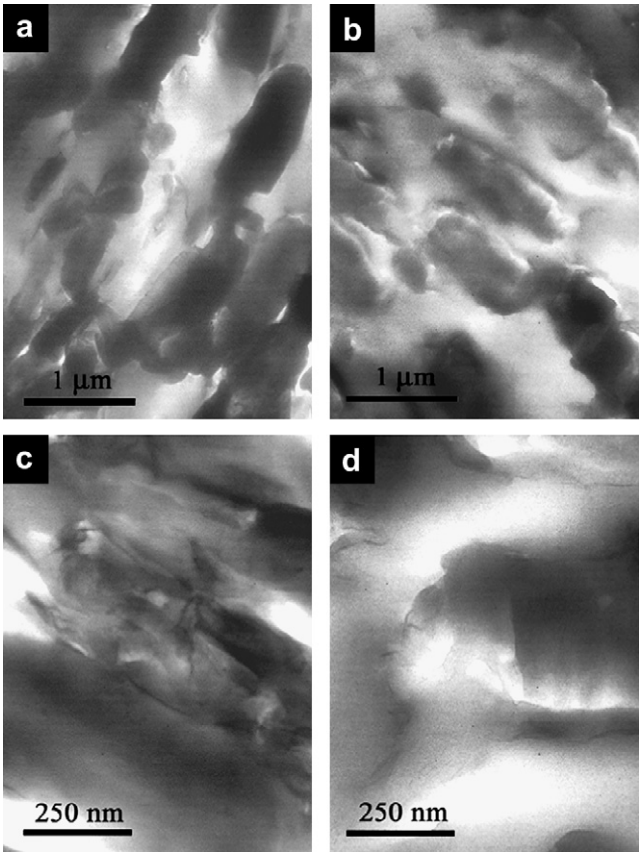

Fig. 1. TEM micrographs of the samples PA25 + 20Clay (a, c) and PA75 + 5Clay (b, d).

The clay, which appears as dark features in the micrographs, results predominantly confined inside well-defined domains representing the minor PA6 phase of the sample PA25 + 20Clay (Fig. 1a). When the host polyamide is the major constituent of the blend, the silicate layers seem gather the interfacial region delineating the contours of the HDPE domains (Fig. 1b). Higher magnifications reveal a scarce degree of exfoliation of the organoclay in both samples, with the presence of distorted tactoids and agglomerated silicate stacks (Fig. 1.c, d). This is in agreement with the results of WAXD analyses, summarized in Table 2 in terms of interlayer spacing between the silicate layers, d_{001}.

The samples PA25 + 20Clay and PA75 + 5Clay exhibit a comparable slight increase of d_{001} with respect to the pristine organoclay, meaning that a small intercalation of polymer chains in between the silicate layers has occurred during the melt mixing. We notice that a similar intercalated structure is observed when the clay is mixed with the neat PA6, whereas the silicate layers collapse when dispersed in the pure HDPE as a consequence of the thermo-degradation of the modifying alkyl ammonium groups of Cloisite® 15 A. This further supports the assumption of preferential location of the filler inside the polyamide phase.

Hereinafter the filled blends will be approximately depicted as two-phase systems constituted by an "unfilled" HDPE phase mixed with an organoclay-rich PA6 phase containing predominantly intercalated organoclay stacks. The impact of such uneven distribution of the filler on the microstructure of the blends was inspected by combining SEM analyses and extraction experiments using selective solvents. We start analyzing the blends in which the wetting polyamide represents the minor phase of the blend. The SEM micrographs showing the microstructural evolutions with increasing the organoclay content are shown in Fig. 2, together with a plot showing the corresponding evolutions of the average size of the inclusions D_v, the circularity factor C and the degree of phase continuity of the minor polyamide phase, φ_{PA6}.

The unfilled sample exhibits globular morphology, the PA6 forming spherical droplets with average diameter of ~10 μm suspended in the HDPE matrix (Fig. 2a). Due to the high interfacial tension, the spherical morphology is the most thermodynamically favored in immiscible blends as it leads to the minimization of the specific interfacial area. In addition, we observe that the poor affinity between the two polymers results in a poor interfacial adhesion. Adding low amounts of organoclay (up to Clay/PA6 = 0.025) causes a substantial reduction of the average drop size, and the circularity of the filled polyamide inclusions decreases slightly (Fig. 2b and c). The microstructure, however, remains globular, as indicated by the relatively low values of φ_{PA6}. Actually, the degree of continuity of the minor phase of a blend with globular morphology should be negligible, but the loss of dispersed particles at the surface of the samples artificially increases the degree of continuity measured through solvent extraction experiments. This sample size effect can be clearly observed in Fig. 3a, showing a detail of the edge of the sample PA25 + 1Clay at the end of the tests.

A surface layer of ~50 μm can be noticed in which the solvent has penetrated passing through surface pores and defects. We remark, however, that the sample size effect tends vanishing when approaching the full phase continuity of the soluble phase [27], so that the high values of φ_{PA6} detected for the samples PA25 + 5Clay and PA25 + 20Clay can be considered reliable, at least within the experimental error.

The high degree of PA6 phase continuity complicates the analysis of the size and shape of the polyamide, so that neither D_v nor C are provided in Fig. 2 for the samples PA25 + 5Clay and PA25 + 20Clay. However, it is interesting to notice a coarsening of the morphology around the onset of PA6 phase continuity, that is when the PA6/Clay ratio is raised up from 0.025 (Fig. 2c) to 0.05 (Fig. 2d). We also remark the elongated shape of the organoclay-rich polyamide domains in the sample PA25 + 5Clay. This is reminiscent of unfilled blends, in which the form factor of the minor phase reaches a minimum at the phase inversion composition [28]. Possible analogies with our nanofilled blends, however, merits further investigations and will be addressed in a next work.

It is important to observe that the high extent of PA6 phase continuity detected for the samples PA25 + 5Clay and PA25 + 20Clay would not be predictable by using the empiric relations and theories generally employed for unfilled blends, in which the phase inversion composition $\Phi_{i,c}$, that is the composition around which co-continuity set up, is simply related to the ratio between the viscosities of the blend constituents, p [29–31]. This is shown in Table 3, were the predictions of some of these relationships are summarized for our systems at $\dot{\gamma} \approx 30 s^{-1}$, that is in the typical range of shear rates attained during extrusion.

The data demonstrate the inadequacy of the models used for unfilled blends. This is not unprecedented, and Li and Shimitzu [17] and Ray et al. [19] similarly observed unexpected occurrence of co-continuity promoted by organoclay. The authors concluded that the mechanism through which nanoparticles promote co-continuity cannot be simply explained in terms of changes in the viscosity of the blend constituents.

The SEM micrographs of the blends with the polyamide as the major constituent are shown in Fig. 4 with varying the organoclay content. In the same figure the evolutions of D_v, C and φ_{HDPE} are reported.

The unfilled blend exhibit globular morphology, whit HDPE droplets of ~10 μm in size suspended in the host PA6 (Fig. 4a). The organoclay promotes a drastic reduction of the average size of the minor phase, which falls down to ~2 μm upon addition of only 1 wt-% of filler with respect to the PA6. Moreover, the presence of elongated HDPE inclusions can be noticed, resulting in a decrease of the average circularity factor (Fig. 4b). This trend continues with increasing the organoclay content (Fig. 4c–e), and the drastic refinement of microstructure makes difficult the estimation of morphological parameters for the sample PA75 + 20Clay. However, differently from what observed in the blends in which the filler enriches the minor phase, we notice that the degree of HDPE phase continuity remains low irrespective of the organoclay content.

The refinement of the morphology noticed in polymer blends filled with organoclay is sometimes explained by invoking some compatibilizing action of the organoclay, which contributes to the formation of *in situ* grafts due to the intercalation of polymer chains into the silicate stacks localized at the interface between the phases [32–34]. Interfacial adhesion, however, would benefit from such a coupling mechanism, whereas a weak interaction seems existing between the HDPE and the filled PA6 of our systems. This is shown in Fig. 5, where the unetched surfaces of the samples PA25 + 5Clay and PA75 + 5Clay are reported.

The microvoids surrounding the minor phase inclusions, as well as the holes due to the removal of dispersed polymer particles during fracture, indicate a scarce adhesion between the phases even for the sample PA75 + 5Clay, in which the filler gathers at the

Table 2
Angular location of the scattering intensity peak, 2θ, and interlayer distances, d_{001}, for the pristine clay, the nanocomposites based on the neat polymers at 5 pphr of clay and the nanocomposite blends PA25 + 20Clay and PA75+5Clay.

Sample	2θ [deg]	d_{001} [nm]
Clay	2.81	3.14
PA25 + 5Clay	2.75	3.21
PA75 + 5Clay	2.63	3.36
HDPE + 5Clay	3.68	2.40
PA + 5Clay	2.57	3.43

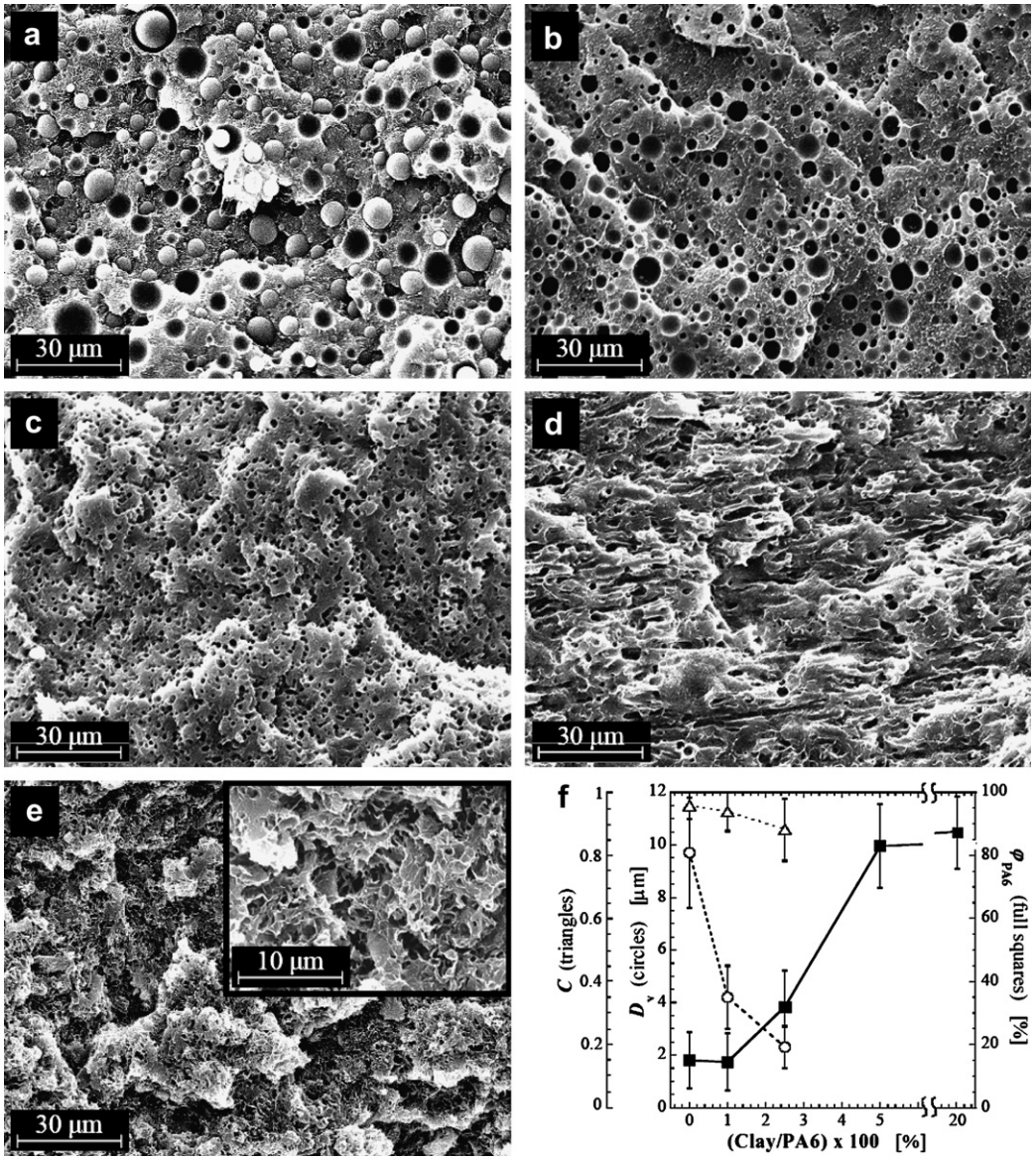

Fig. 2. SEM micrographs of the sample PA25 (a) and the blends having HDPE as the major constituent with different amount of filler: PA25 + 1Clay (b), PA25 + 2.5Clay (c), PA25 + 5Clay (d), and PA25 + 20Clay (e). The surfaces of the filled blends were etched with formic acid in order to remove the minor PA6 phase. The average size, D_v, circularity, C and degree of continuity, φ_{PA6}, of the minor PA6 phase are shown in (f) as a function of filler content.

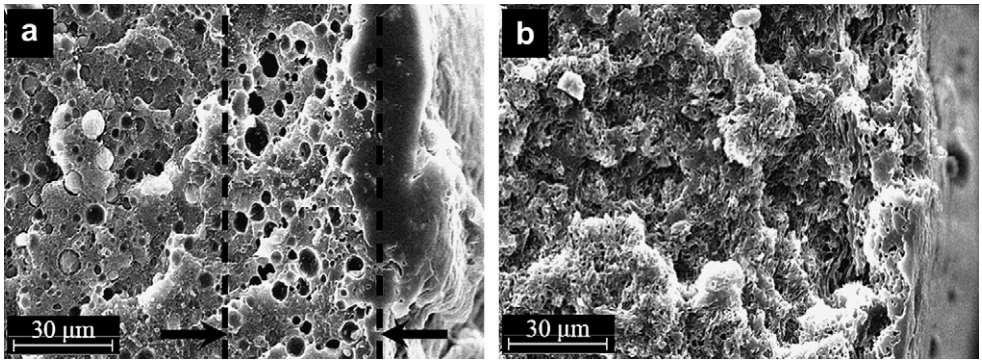

Fig. 3. SEM micrographs showing the edge of samples PA25 + 1Clay (a) and PA25 + 20Clay (b) at the end of the solvent extraction experiments. The surface layer in which the solvent has penetrated removing the soluble minor phase is highlighted in (a).

Table 3
Predictions of the volume fraction of HDPE at co-continuity computed at $\dot{\gamma} = 30s^{-1}$ using the relationships by Ho et al. [29], Utracki [30] and Miles and Zurek [31].

	Ho et al [29]	Utracki [30]	Miles and Zurek [31]
Constituents		$\Phi_{HDPE,c}$ [Vol-%]	
HDPE, PA6	38	38.5	27
HDPE, PA6 + lClay	38	38	25
HDPE, PA6 + 2.5Clay	37.5	37	23
HDPE.PA6 + 5Clay	36.5	35	21.5
HDPE, PA6 + 20Clay	35.5	33.5	20

interfacial region (see Fig. 1b). A similar conclusion was drawn in our previous paper, where the coupling mechanism related to the organoclay was compared to that of a chemical compatibilizer precursor [24]. Therefore, the weak interfacial adhesion shown in Fig. 5 suggests that the changes in the microstructure of the blends should be mainly ascribed to the changes in the properties of the filled polyamide, and specifically of its melt state relaxation dynamics, the interface properties playing a minor role in determining the observed effects.

3.2. Hypotheses about the filler-induced morphological changes

As discussed above, the high degree of continuity of the organoclay-rich PA6 phase in the samples PA25 + 5Clay and PA25 + 20Clay cannot be predicted by invoking rules simply based on the ratio between the viscosities of the constituents. However, the presence of nanoparticles inside the polyamide phase of the blend not only affects the steady-state shear viscosity of the host polymer, but also its viscoelastic behavior. In our previous paper we found that the linear viscoelastic behavior of the sample PA25 + 20Clay is reminiscent of that of single-phase polymer-layered silicate nanocomposites [24]. This has been interpreted as a direct consequence of the high degree of continuity of the organoclay-rich PA6 phase, which governs the low-frequency viscoelastic response of the blend by acting in parallel with the major HDPE phase. In order to investigate about possible relationships between the unexpected occurrence of co-continuity and the changes in linear viscoelastic properties of the minor phase of filled PA6 with varying the filler content, the frequency dependence elastic moduli, G', and loss factors, $\tan\delta = G''/G'$, are shown in Fig. 6

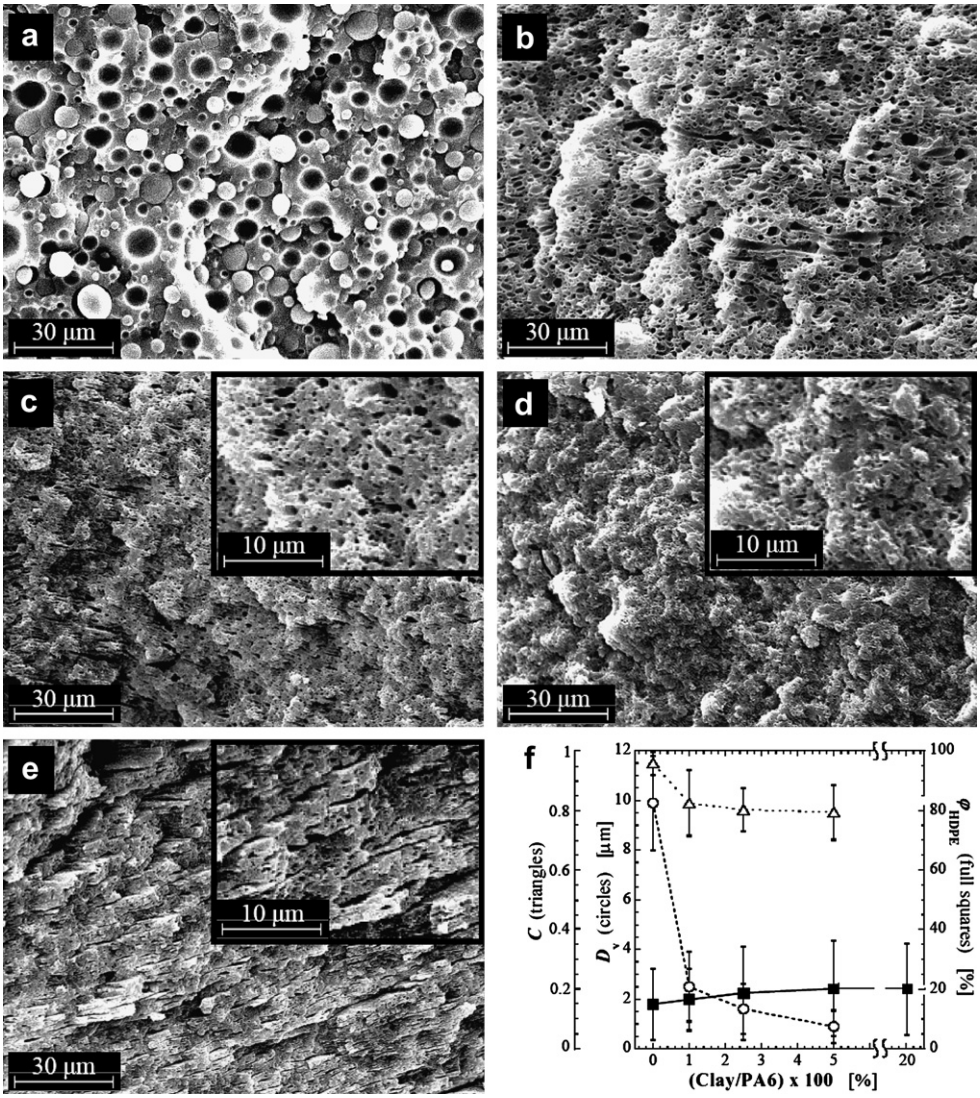

Fig. 4. SEM micrographs of the sample PA75 (a) and the blends having PA6 as the major constituent with different amount of filler: PA75 + 1Clay (b), PA75 + 2.5Clay (c), PA75 + 5Clay (d), and PA75 + 20Clay (e). The minor HDPE phase was selectively removed from the surfaces of the filled blends using boiling toluene. The average size, D_v, circularity, C and degree of continuity, φ_{HDPE}, of the HDPE minor phase are shown in (f) as a function of filler content.

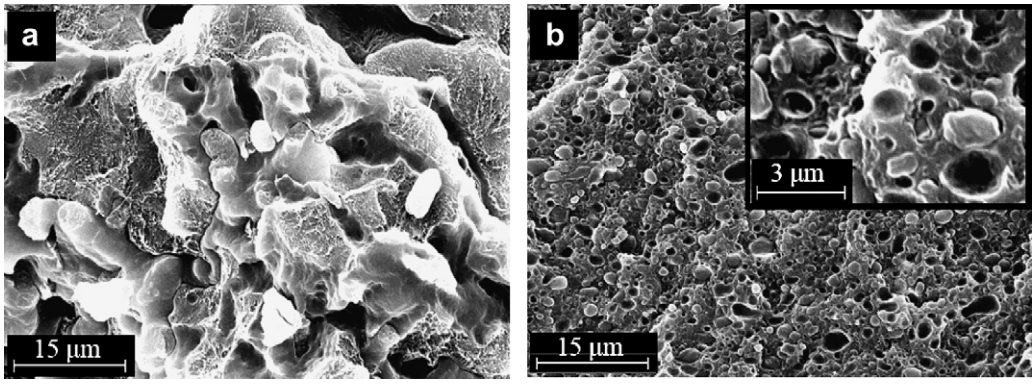

Fig. 5. SEM micrographs showing the unetched surfaces of the sample PA25 + 5Clay (a) and PA75 + 5Clay (b).

for the neat PA6 and its nanocomposites at the same Clay/PA6 ratio of the studied blends.

The unfilled polymer exhibits a predominantly viscous feature (tan $\delta > 1$) in the whole range of frequency investigated, approaching terminal behavior ($G' \sim \omega^2$ and tan $\delta \sim \omega^{-1}$) at low ω. The decrease of tan δ with increasing the organoclay content indicates that the filler enhances the elastic connotation of the PA6. The whole trend, however, remains similar to that of the unfilled polyamide up to Clay/PA6 ratio of 0.025, while a clear rheological transition occurs when the Clay/PA6 ratio is raised up to 0.05. Specifically, the samples PA + 5Clay and PA + 20Clay exhibit a weak power law dependences of G' on ω, and a substantial frequency-independence of the loss factor tan δ. Such a behavior is reminiscent of systems around the gel point. The rheological response of a gel is determined by a space spanning network structure, either chemical or physical in nature, which is responsible for the broadening and slackening of relaxation dynamics [35]. In the studied blends, the observed rheological transition could be ascribed to the structuring of the organoclay near some critical filler loading between 2.5 and 5 parts of clay with respect to PA6. Similar conclusions were recently drawn by Ayyer and Leonov, who found gel-like behavior at lower filler contents probably due to a higher degree of exfoliation of the silicate platelets in their *in situ* polymerized PA6/Clay nanocomposites [36].

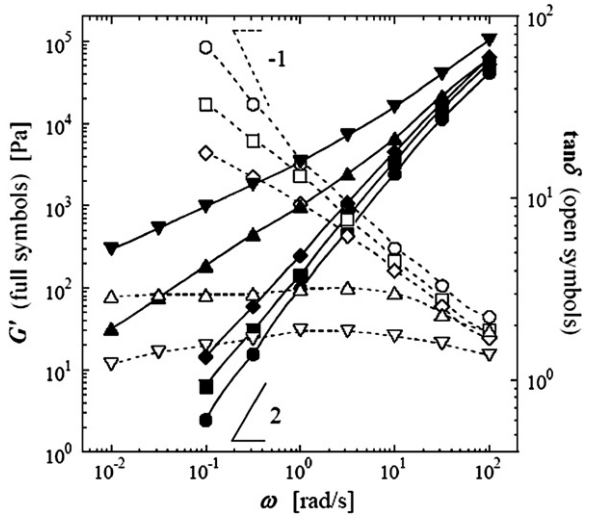

Fig. 6. Elastic modulus G' (full symbols, left axis) and loss factor tan δ (open symbols, right axis) of the neat polyamide (circles) and the PA6-based nanocomposites at different Clay/PA6 ratio: 0.01 (squares), 0.025 (diamonds), 0.05 (triangles), and 0.20 (reverse triangles).

It is noteworthy to remark that the samples PA + 5Clay and PA + 20Clay, that is the blends in which the organoclay-rich PA6 minor phase shows a gel-like behavior, exhibit a highly interpenetrated microstructure in spite of the relatively low content of the minor phase. Such a correspondence, together with the evidences emerged from morphological analyses, suggests the simplified picture schematically depicted in Fig. 7.

We start discussing the case of the blends in which the filler distributes inside the minor phase (Fig. 7a–c). When small amounts of organoclay are added, that is for filler loadings below the critical threshold for the structuring of the network, the polyamide encapsulates the organoclay stacks finely dispersed during the melt mixing. This results in a general refinement of the microstructure that, however, remains globular. In addition, since coalescence involves flows inside the merging droplets, we observe that coarsening phenomena could result hindered due to the increased viscosity of the organoclay-rich polyamide inclusions. With increasing the filler content, the polyamide phase becomes continuous in spite of its relatively low content. As previously discussed, this finding cannot be explained in the context of bulk continuum properties, such as altered viscosity ratios in the presence of nanoparticles. Since the sudden increase of φ_{PA6} is coupled to the rheological transition of the filled polyamide, we can speculate that a double percolating network forms above a critical filler content, in which the polyamide gets continuous as it coats a space spanning organoclay network. According to this simplified picture, the filler seems guiding the space arrangement of the minor polyamide phase in the blends. This is in agreement with computer simulations performed by Peng et al. [37], who demonstrated that nanoscale rods promotes co-continuity in binary mixtures as a result of a dynamic interplay among preferential adsorption of the minority component onto the mobile nanoparticles, phase-separation and anisotropic interparticle interactions. Besides driving the structural evolutions of the fluids, however, the authors stress that the filler is also physically moved by osmotic effects resulting from the phase-separation process. Although the occurrence of such a mechanism cannot be excluded in the studied blends, the complex thermo-mechanical history taking place during the processing makes it difficult to separate and quantify the roles of filler, phase-separation and mechanical mixing in assisting the formation of co-continuity.

When the filler locates inside the major phase, a drastic reduction of the size of the dispersed phase occurs upon addition of even small amounts of organoclay (Fig. 7d and f). Coalescence suppression is often proposed as the dominant mechanism on the basis of the morphology refinement in organoclay-filled polymer blends [11,38,39]. Basically, coarsening is hindered because of the platelet-like structure of the filler, which acts as physical barriers that prevent the coalescence of colliding droplets during the melt mixing.

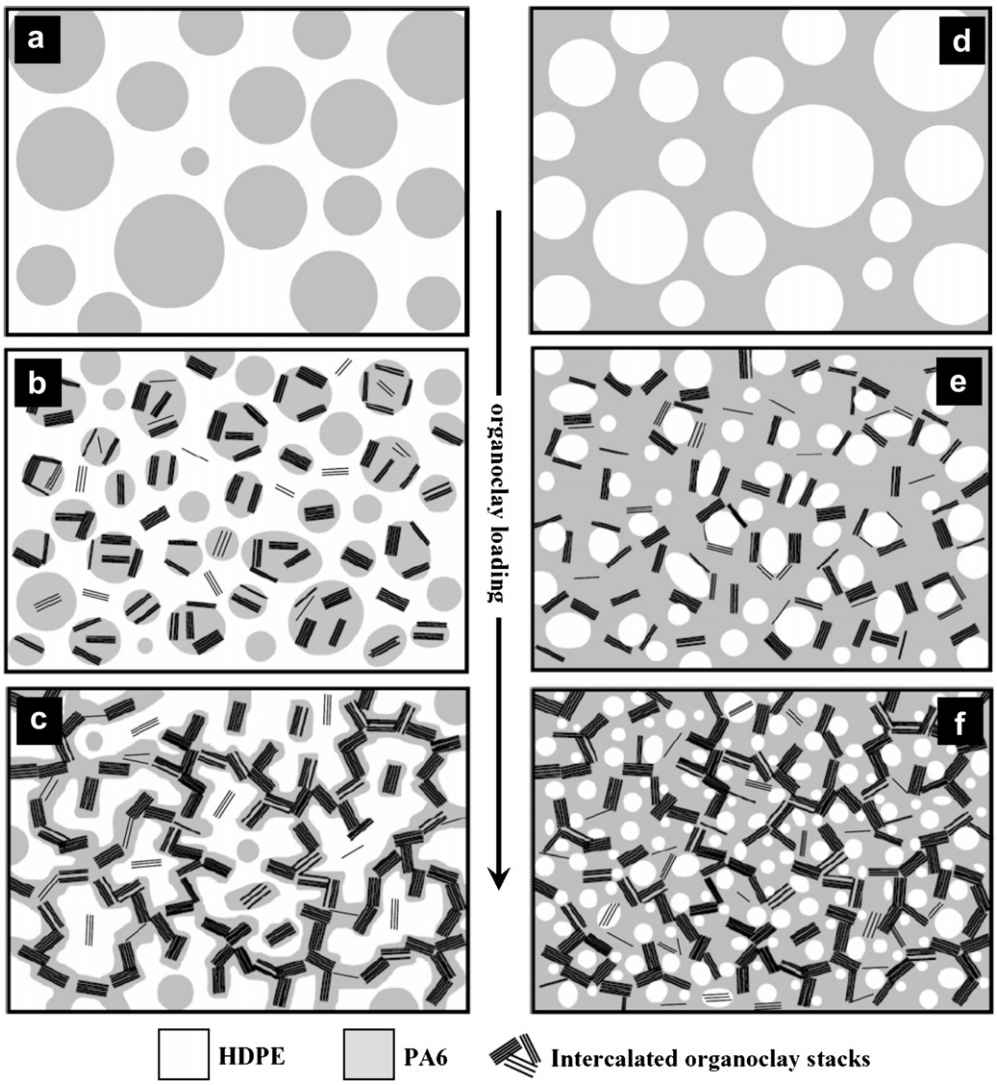

Fig. 7. Schematic illustration of the evolutions of the microstructure in the blends with polyamide as the minor (a–c) or major (d–f) phase as a result of the addition of organoclay.

The occurrence of such a mechanism is compatible with the finding that the silicate layers tend accumulating in the interfacial region (see Fig. 1b). As schematically shown in Fig. 6, we expect that the morphology refinement would be weakly dependent on the degree of dispersion of the organoclay. In particular, tiny droplets of the minor phase may result trapped by the physical network of particles when the concentration of solid is above the critical threshold for its structuring. We cannot exclude, however, that other phenomena could combine to bring about the refinement of microstructure. In particular, we observe that the increased viscosity of the filled matrix may hinder the flows involved in the coalescence processes. Moreover the enhanced elasticity of the minor organoclay-rich polyamide phase (see Fig. 6) could also contribute to reduce the critical conditions for droplet break up [40].

3.3. Dynamic-mechanical analyses

The changes in microstructure promoted by the filler are expected to affect remarkably the macroscopic behavior of the blends. The results of dynamic-mechanical tests are shown in Fig. 8, where the storage modulus E' and the loss factor $\tan\delta = E''/E'$ at 1 Hz are reported as a function of temperature for the neat polymers, the unfilled blends and the blends at Clay/PA6 = 0.20.

As expected in the light of the microstructural analyses, the dynamic-mechanical behavior of the unfilled blends, both having globular morphology, is essentially governed by the matrix: the modulus of the sample PA25 drops down at ~130 °C due to the melting of the HDPE, while the blend PA75 exhibits the same two main transitions of the PA6, that is the β-relaxation around −60 °C (movement of chain segments and amide groups) and the glass transition at ~60 °C. The organoclay has a marginal effect on the glass transition temperature of the host PA6, whereas it promotes increases of the glassy modulus of the blends of order of 20–30% (inset of Fig. 8). It is important to notice that the enhancement of E' of the sample PA25 + 20Clay, ensured by a whole organoclay content equal to one third of that of the sample PA75 + 20Clay (see Table 1), stems from the combination of the action of the filler, selectively reinforcing the minor polyamide phase, and the highly co-continuous microstructure, which ensures that both phase contribute to the mechanical strength irrespective of the efficiency of the stress transfer across the interface [41,42]. The strengthening effect of the filler persists even at high temperature. However, whereas the overall behavior of the sample PA75 + 20Clay resembles that of its unfilled counterpart, the blend PA25 + 20Clay exhibits a small but finite plateau of E' even above the melting of the major polyethylene

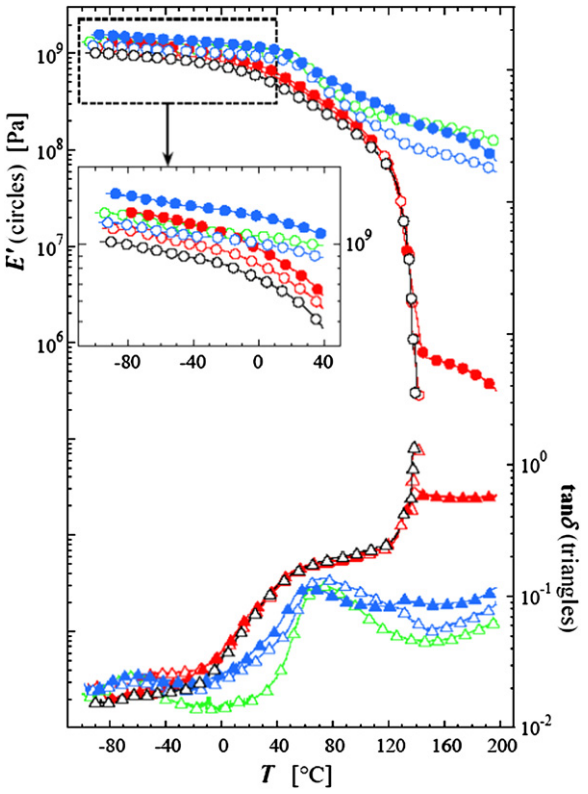

Fig. 8. Storage modulus E' (circles, left axis) and loss factor tan δ (triangles, right axis) at 1 Hz as a function of temperature for various samples: HDPE (black), PA6 (green), PA25 (red, open symbols), PA25 + 20Clay (red, full symbols), PA75 (blue, open symbols), and PA75 + 20Clay (blue, full symbols) (For interpretation of the references to colour in this figure legend, the reader is referred to the web version of this article).

phase, which is due to the presence of the continuous structure of filled polyamide.

The ability of such a tenuous network of keep bearing the stress even after the melting of the HDPE has a noteworthy consequence in terms of mechanical strength at high temperature. This can be clearly appreciated in Fig. 9, where the pictures of the samples PA25 and PA25 + 20Clay at the end of the DMA tests are shown.

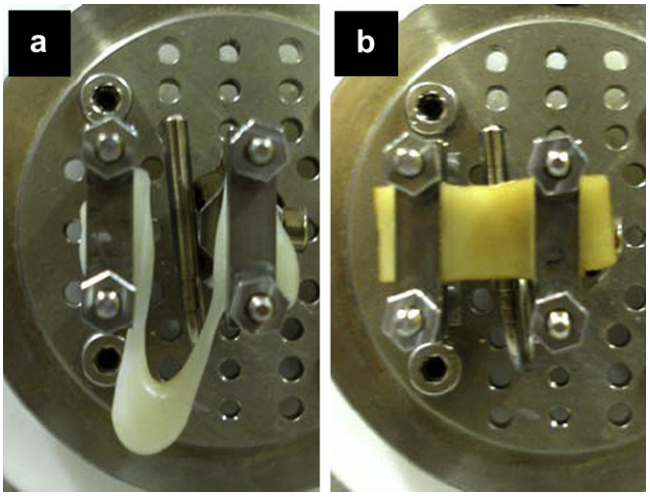

Fig. 9. Pictures of the samples PA25 (a) and PA25 + 20Clay (b) at the end of the DMA tests. The maximum temperatures reached during experiments were ~130 °C for (a) and ~200 °C for (b).

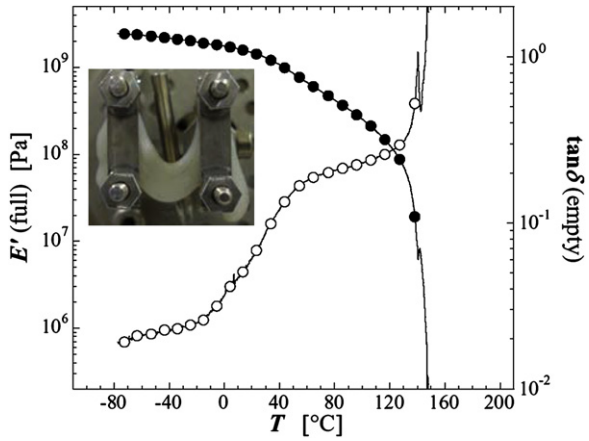

Fig. 10. Storage modulus E' (full circles, left axis) and loss factor tan δ (empty circles, right axis) at 1 Hz as a function of temperature for the samples HDPE + 5Clay. The picture shows the sample soon after the end of the test, that is at ~150 °C.

The unfilled blend softens as soon as the HDPE starts melting, dripping between the clamps at ~130 °C in spite of the rigid but isolated droplets of PA6 embedded in the matrix. Instead, the filled sample keeps its structural integrity up to ~200 °C, that is up to the onset of the melting of the filled PA6 framework. We emphasize that the filler by itself is not able to explain the observed enhancement of the softening temperature, which instead originates from the synergism between the intrinsic reinforcing action of the particles and their ability in promoting the continuity of the high-melting-temperature PA6 phase. This is shown in Fig. 10, where the temperature dependence of E' and tan δ are reported for a sample HDPE + 5Clay, that is a nanocomposite based on the single polyolefin filled with the same amount of filler as the sample PA25 + 20Clay.

The nanocomposite exhibits an improved glassy modulus with respect to the neat HDPE, but its whole behavior during the temperature scan remains essentially unaltered and the sample collapses soon after the melting of the polymer matrix.

Our results confirm the great potentialities offered by the addition of nanoparticles to multiphase polymeric systems, in which rather than the mere capitalization of the filler properties to improve the final performances of the composite, new properties and optimized behaviors can be promoted by means of the manipulation and control of the material nano- and micro-structure.

4. Conclusions

The effect an organomodified clay on the morphology and properties of two HDPE/PA6 blends at opposite composition was investigated with varying the filler content. As the filler tends enriching preferentially the more hydrophilic polyamide phase, different effects on the microstructure of the blends were noticed depending on whether the host PA6 represents the major or the minor blend constituent. In the former case, an abrupt reduction of the average size of the dispersed polyethylene inclusions was noticed even for low filler loadings. This finding was mainly ascribed to the inhibition of coalescence ensured by the platelet-like structure of the organoclay stacks, which act as physical barrier that hinder the merging of colliding droplets during the melt mixing. When the filler is confined inside the minor constituent of the blend, two situations have been observed: at low filler contents, the organoclay causes a gradual refinement of the morphology, which, however, remains globular; for filler loading higher than

a critical threshold, the filled polyamide assembles into a highly continuous structure finely interpenetrated with the major polyethylene phase. The filler content at which such a morphological transition occurs corresponds to that at which a rheological transition from a liquid- to gel-like behavior takes place in the filled polyamide. This has suggested a simplified mechanism according to which the filler seems play a major role in driving the spatial arrangement of the wetting polymer. The ability of the filler of influencing the blend microstructure can be exploited in order to enhance relevant technological properties of the materials. In particular, we found that the filled blends having polyamide as the minor constituent preserve their structural integrity up to temperature well above the melting of the major polyethylene phase owing to the presence of the tenuous but continuous framework of filled polyamide.

References

[1] Ryan AJ. Nat Mater 2002;1:8–10.
[2] Utracki LA. Commercial polymer blends. London: Chapman and Hall; 1998 [Chapter 6].
[3] Pötschke P, Paul DR. Polym Rev 2003;43:87–141.
[4] Kim BJ, Fredrickson GH, Hawker CJ, Kramer EJ. Langmuir 2007;23:7804–9.
[5] Dintcheva NTz, Filippone G, La Mantia FP, Acierno D. Polym Degrad Stab; 2010. doi:10.1016/j.polymdegradstab.2009.12.021.
[6] Hillmyer MA. Adv Polym Sci 2005;190:137–81.
[7] Willemse RC, Posthuma de Boer A, van Dam J, Gotsis AD. Polymer 1999;40 (4):827–34.
[8] Lyngaae-Jorgensen J, Utracki LA. Polymer 2003;44:1661–9.
[9] Elias L, Fenouillot F, Majesté JC, Cassagnau P. Polymer 2007;48:6029–40.
[10] Ray SS, Pouliot S, Bousmina M, Utracki LA. Polymer 2004;45:8403–13.
[11] Khatua BB, Lee DJ, Kim HY, Kim JK. Macromolecules 2004;37:2454–9.
[12] Chow WS, Mohd Ishak ZA, Karger-Kocsis J. Macromol Mater Eng 2005;290: 122–7.
[13] Lee MH, Dan CH, Kim JH, Cha J, Kim S, Hwang Y, Lee CH. Polymer 2006;47:4359–69.
[14] Hong JS, Kim YK, Ahn KH, Lee SJ, Kim C. Rheol Acta 2007;46:469–78.
[15] As'habi L, Jafari AH, Bahaei B, Khonakdar HA, Pötschke P, Böhme F. Polymer 2008;49:2119–26.
[16] Li Y, Shimizu H. Polymer 2004;45:7381–8.
[17] Li Y, Shimizu H. Macromol Rapid Commun 2005;26:710–5.
[18] Wu D, Zhou C, Zhang M. J Appl Polym Sci 2006;102:3628–33.
[19] Ray SS, Bandyopadhyay J, Bousmina M. Macromol Mater Eng 2007;292:729–47.
[20] Zou H, Ning N, Su R, Zhang Q, Fu Q. J Appl Polym Sci 2007;106:2238–50.
[21] Lee SH, Kontopoulou M, Park CB. Polymer 2010;51:1147–55.
[22] Fenouillot F, Cassagnau P, Majesté J-C. Polymer 2009;50:1333–50.
[23] Manias E. Nat Mater 2007;6:9–11.
[24] Filippone G, Dintcheva NT, Acierno D, La Mantia FP. Polymer 2008;49 (5):1312–22.
[25] Pernot H, Baumert M, Court F, Leibler L. Nat Mater 2002;1:54–8.
[26] Galloway JA, Macosko CW. Polym Eng Sci 2004;44(4):714–27.
[27] Galloway JA, Koester KJ, Paasch BJ, Macosko CW. Polymer 2004;45:423–8.
[28] Steinmann S, Gronski W, Friedrich C. Polymer 2001;42(15):6619–29.
[29] Ho RM, Wu CH, Su AC. Polym Eng Sci 1990;30(9):511–8.
[30] Utracki LA. J Rheol 1991;35:1615–37.
[31] Miles IS, Zurek A. Polym Eng Sci 1988;28:796–805.
[32] Si M, Araki T, Ade H, Kilcoyne ALD, Fisher R, Sokolov JC, et al. Macromolecules 2006;39(14):4793–801.
[33] Fang Z, Xu Y, Tong L. Polym Eng Sci 2007;47:551–9.
[34] Gcwabaza T, Sinha Ray S, Focke WW, Maity A. Eur Polym J 2009;45 (2):353–67.
[35] Holly EE, Venkataraman S, Chambon F, Winter HH. J Non-Newtonian Fluid Mech 1988;27:17–26.
[36] Ayyer RK, Leonov AI. Rheol Acta 2004;43:283–92.
[37] Peng G, Qiu F, Ginzburg VV, Jasnow D, Balazs AC. Science 2000;228: 1802–4.
[38] Lee H, Fasulo PD, Rodgers WR, Paul DR. Polymer 2005;46(25):11673–89.
[39] Kelnar I, Khunova V, Kotek J, Kapralkova L. Polymer 2007;48:5332–9.
[40] Mighri F, Carreau PJ, Ajji A. J Rheol 1998;42(6):1477–90.
[41] Veenstra H, Verkooijen PCJ, van Lent BJJ, van Dam J, de Boer AP, Nijhof APHJ. Polymer 2000;41:1817–26.
[42] Filippone G, Dintcheva NT, La Mantia FP, Acierno D. J Polym Sci Part B Polym Phys 2010;48(5):600–9.